

1 **Supplementary Materials**  
2 **for**

3 **Exploring the effects of operational mode and microbial interactions on**  
4 **bacterial community assembly in a one-stage partial-nitritation anammox**  
5 **reactor using integrated multi-omics**

6 Yulin Wang<sup>1</sup>, Qigui Niu<sup>2</sup>, Xu Zhang<sup>3</sup>, Lei Liu<sup>1</sup>, Yubo Wang<sup>1</sup>, Yiqiang Chen<sup>1</sup>, Mishty Negi<sup>1</sup>,  
7 Daniel Figeys<sup>3</sup>, Yuyou Li<sup>4</sup>, Tong Zhang<sup>1\*</sup>

8 <sup>1</sup>Environmental Biotechnology Laboratory, Department of Civil Engineering, The University of Hong  
9 Kong, Pokfulam Road, Hong Kong

10 <sup>2</sup>School of Environmental Science and Engineering, Shandong University, 27# Shanda South Road,  
11 Jinan 250100, China

12 <sup>3</sup>Department of Paediatrics, CHEO Inflammatory Bowel Disease Centre and Research Institute,  
13 University of Ottawa, Ottawa, ON, Canada

14 <sup>4</sup>Department of Civil and Environmental Engineering, Graduate School of Engineering, Tohoku  
15 University 6-6-06 Aoba, Aramaki, Aoba-ku, Sendai 980-8579, Japan

16 E-mail zhangt@hku.hk; Tel. 852-28578551; Fax 852-25595337.  
17

18 This file includes:

19 **Methods**

20 S1 Reactor operation

21 S2 DNA and RNA extraction and sequencing

22 S3 Protein extraction, trypsin digestion, and mass spectrometry analysis

23 S4 Metagenomic and metatranscriptomic analysis

24 S5 Metaproteomic analysis

25 S6 Peptidases identification

26 **Figures**

27 Figure S1. Variation of nitrogen components in the influent (ammonium-nitrogen) and effluent  
28 (ammonium-nitrogen, nitrite-nitrogen and nitrate-nitrogen) and nitrogen removal rate of the  
29 PNA reactor.

30 Figure S2. Color changes of sludge in the studied one-stage PNA reactor.

31 Figure S3. Characterization of the anammox granules on day 308. a, Image of the anammox  
32 granules. b, Light microscope of the anammox granules. c, Size distribution of the anammox  
33 sludge.

34 Figure S4. Microbial community structures in the anammox sludge samples. The relative  
35 abundance of taxonomic groups is estimated based on the sequence percentage of the total 16S  
36 rRNA sequences in each activated sludge sample at phylum (a) and genus levels (b). The genera  
37 that have relative abundance <1% are assigned to the category of “Others”. The taxonomy was  
38 presented at the lowest level that can be identified.

39 Figure S5. Plot of differential coverage binning approach, the corresponding relationships  
40 between IDs and MAGs information are listed in Table S1. The coverage of x-axis represents  
41 the mapping coverage of metagenomic data originated from the samples taken on days 204,  
42 210 and 213, and the y-axis represents the mapping coverage of metagenomic data originated

43 from the sample of seed sludge.

44 Figure S6. Comparison of relative abundance in different anammox sludge samples. The  
45 relative abundance (normalized by the genome size) represents the ratio of recruited  
46 metagenomic sequences of one given MAG to the total recruited metagenomic sequences of all  
47 the recovered MAGs.

48 Figure S7. Relative abundance (weighted) of bacterial community composition assessed by  
49 identified protein. S1-1, S1-2, and S1-3 are the technical repeats of sample S1.

50 Figure S8. Identified proteins ( $\log_{10}(\text{LFQ intensity})$ ) for nitrogen metabolism in AOB and  
51 anammox bacteria. Proteins that could be assigned to specific ORFs of recovered MAGs were  
52 represented with MAG ids, the proteins with best hits to the UniProt database were represented  
53 with taxonomy (genus level). Differential protein expressions are marked with red asterisk  
54 (ratio  $>1.2$  or  $<0.83$  coupled with a P value  $<0.05$ ).

55 Figure S9. Relative gene expression of amino acid transporters in CFX1 and identified  
56 peptidases in dominant organisms. (a) Relative gene expression of amino acid and peptide  
57 transporters in CFX1 throughout the time series, and aligned with the corresponding gene loci.  
58 The wiggly lines indicate ends of the contig, and parallel double lines show a break in locus  
59 organization. Subfamily types of the encoded transporters are represented by color. (b) ORFs  
60 of dominant organisms (relative abundance  $>1\%$ ) were firstly annotated using MEROPS  
61 database, and the potential peptidases were further confirmed by CD search. The locations of  
62 peptidases were predicted by PSORT, and the extracellular, outer membrane and periplasmic  
63 peptidases are shown in this figure. (c) Dynamics of highly expressed genes throughout the  
64 time series.

65 Figure S10. Gene expression profiles of ten selected metabolic pathways in the dominant  
66 autotrophs. These were estimated based on the ratios of recruited metatranscriptomic sequences  
67 of genes involved in selected pathways to the total recruited metatranscriptomic sequences of  
68 the corresponding MAGs.

69

## 70 **Methods**

### 71 **S1 Reactor operation**

72 The reactor that was operated in the present study was a modified fermentor (Sartorius  
73 BIOSTAT B, Goettingen Germany). At Stage I, the reactor was operated in continuous mode at  
74 an HRT of 12 hours, which was well controlled by a computer system equipped with pH, level  
75 and DO meters. In order to recover the nitrogen removal rate and avoid the loss of anammox  
76 sludge, the operating mode was adjusted to a sequencing batch reactor (SBR) operating mode.  
77 The PNA reactor was operated with 8 hours, and a fixed exchange ratio of 50% was employed  
78 to achieve an HRT of 16 hours. The 8-hour cycle included 6 min feed phase, 450 min reaction  
79 phase (divided into 3 aerated and 3 non-aerated phases), 4 min settling phase [1], 10 min  
80 discharge phase and a 10 min idle phase (Fig. 1). The temperature of the reactor was operated  
81 at 30°C, and the pH was maintained at between 7.8 and 8.1. The stirrer was set at a speed of 80  
82 rpm to ensure the homogeneous distribution of substrate and biomass and to avoid the  
83 disturbance of anammox granules. The reactor was aerated with large air bubbles during the  
84 aeration phases to avoid excessive dissolved oxygen, which would result in an oxygen-deficient  
85 condition that DO could not be detected in the whole reaction cycle. The reactor was fed with  
86 synthetic influent, containing ammonium as the single nitrogen source, mineral salt, and no  
87 organic carbon. The ammonium concentration was decreased from 250 mg-N/L to 200 mg-N/L  
88 on the 16<sup>th</sup> day and increased to 250 mg-N/L on the 171<sup>st</sup> day. The mineral medium in the  
89 synthetic influent was made as follows: 40 mg/L KH<sub>2</sub>PO<sub>4</sub>, 107 mg/L Na<sub>2</sub>HPO<sub>4</sub>·12H<sub>2</sub>O, 150  
90 mg/L CaCl<sub>2</sub>·2H<sub>2</sub>O, 25 mg/L MgCl<sub>2</sub>·6H<sub>2</sub>O, and 1 mL/L trace element (8.304 g/L  
91 Na<sub>2</sub>·EDTA·2H<sub>2</sub>O, 5.000 g/L FeSO<sub>4</sub>·7H<sub>2</sub>O, 0.215 g/L ZnSO<sub>4</sub>·7H<sub>2</sub>O, 0.120 g/L CoCl<sub>2</sub>·6H<sub>2</sub>O,  
92 0.495 g/L MnCl<sub>2</sub>·4H<sub>2</sub>O, 0.125 g/L CuSO<sub>4</sub>·5H<sub>2</sub>O, 0.110 g/L Na<sub>2</sub>MoO<sub>4</sub>·2H<sub>2</sub>O, 0.095 g/L  
93 NiCl<sub>2</sub>·6H<sub>2</sub>O, 0.078 g/L Na<sub>2</sub>SeO<sub>3</sub>, 0.007 g/L H<sub>3</sub>BO<sub>4</sub>) [2].

### 94 **S2 DNA and RNA extraction and sequencing**

95 For the triplicate samples from 3 independent reaction cycles, 1.5 mL of anammox sludge (3500  
96 mg volatile solids /L, VS/L) was used to extract the total RNA with MoBio RNA PowerSoil

97 total RNA isolation kit (MoBio, USA), resulting in 24 total RNA samples for  
98 metatranscriptomic sequencing. The corresponding DNA was then eluted using the RNA  
99 PowerSoil DNA elution accessory kit (MoBio, USA), and DNA samples obtained from each  
100 reaction cycle (8 samples) were equally mixed based on the DNA concentration, resulting in 3  
101 DNA samples for metagenomic sequencing. Quantities and qualities of genomic DNA and total  
102 RNA were checked using the Nanodrop ND 1000 (Thermo Fisher Scientific, USA) and Agilent  
103 2100 Bioanalyzer (Agilent, USA).

104 For the extracted total RNA samples, the residual genomic DNA was removed using PureLink  
105 DNase set (Life Technologies, NY, USA), and the non-rRNA were enriched using Ribo-Zero  
106 rRNA Removal Kit for bacteria (Illumina, CA, USA). Reverse transcription was performed  
107 using SuperScript II Reverse Transcriptase (Life Technologies, NY, USA) with an initial  
108 annealing of random hexamers (Thermo Fisher Scientific, PA, USA), and the complementary  
109 DNA (cDNA) was purified with Ampure XP beads (Beckman Coulter, IN, USA), followed by  
110 second-strand synthesis. The finally constructed double-stranded cDNA fragments were further  
111 processed for library construction.

### 112 **S3 Protein extraction, trypsin digestion, and mass spectrometry analysis**

113 All samples were concentrated to 7000 mg VS/L for protein extraction. The protein extraction  
114 was extracted using the B-PER extraction method. 1.5 mL sludge sample was centrifuged at  
115 15,000 g for 15 min at 4 °C. Discarded the supernatant and resuspended the pellet in 1 mL of  
116 B-PER extraction buffer (77 mg of dithiothreitol (DTT), 1 tablet of Complete Mini protease  
117 inhibitor, 10 mL of B-PER reagent) [3, 4]. Samples were placed at -80 °C for 1 hr, thawed and  
118 incubate for 1 hr on ice. Cells are lysed by bead beating (4 cycles for 40 s at 6 m/s with 2 min  
119 breaks on ice) using FastPrep-24™ Homogenizer (MP Biomedicals, California, USA). Samples  
120 were centrifuged at 15,000 g for 15 min at 4°C to remove cell debris and the supernatant was  
121 transferred to a fresh 2.0 mL tube. The 50:50:0.1 acetone/ethanol/acetic acid was added to the  
122 supernatant (1.5 mL) and incubated at 4 °C for overnight to precipitate proteins. Centrifuge the  
123 samples at 15,000 g for 20 min at 4 °C to collect the protein pellets. The obtained protein pellets  
124 were washed thrice in 200 µL 100% ice-cold acetone and centrifuged at 20,000 g at 4 °C for 20

125 min every time[5]. Remove the supernatant and freeze-dry (Heto Drywinner 3), the dried  
126 samples were stored at -80 °C until LC-MS analysis. For the tryptic digest, 50 µg proteins were  
127 reduced and alkylated with 10 mM dithiothreitol and 20 mM iodoacetamide, respectively. One  
128 microgram of trypsin (Worthington Biochemical Corp., Lakewood, NJ) was then added to each  
129 sample for in-solution trypsin digestion at 37 °C overnight with agitation.

130 The separation of tryptic peptides was performed on an analytical column (75 µm × 50 cm)  
131 packed with reverse phase beads (1.9 µm; 120-Å pore size; Dr. Maisch GmbH, Ammerbuch,  
132 Germany) with 4-hour LC gradient from 5 to 35% acetonitrile (v/v) at a flow rate of 200 nl/min.  
133 The instrument method consisted of one full MS scan from 300 to 1800 m/z followed by data-  
134 dependent MS/MS scan of the 12 most intense ions. A dynamic exclusion repeat count of 2 and  
135 repeat exclusion duration of 30 s was used for ion selections. All data were recorded with the  
136 Xcalibur software and exported as .raw format for further metaproteomic data analysis.

#### 137 **S4 Metagenomic and metatranscriptomic analysis**

138 The shotgun sequences were quality controlled using CLC Genomics Workbench (v6.04,  
139 CLCBio, Qiagen) to get clean reads (average Q value >30) for downstream *de-novo* assembly.  
140 The clean reads were co-assembled using CLC's *de novo* assembly algorithm (CLC Genomics  
141 Workbench v6.04, CLCBio, Qiagen) with a *k*-mer of 35 and a minimum scaffold length of 1  
142 Kbp. To get the coverage of scaffolds for genome binning, the metagenomic reads from  
143 anammox sludge samples (seed vs integrated data of days 204, 210, and 213) were mapped to  
144 co-assembled scaffolds with a similarity fraction of 90% over an 80% read length. Mapping  
145 was performed with random nonspecific matches if a read aligned to more than one position  
146 with equally good scores. The mapping results were then used to calculate the average coverage  
147 of assembled scaffolds. Two-dimensional coverage binning approach was used to retrieve the  
148 MAGs of the microbial community member in anammox sludge [6].

149 After trimming the 15 bp low-quality region at the 3' end, the paired-end metatranscriptomic  
150 reads were quality filtered. The high quality (average quality score >30) metatranscriptomic  
151 reads were subsequently screened using SortMeRNA v2.1 to remove the rRNA sequences based

152 on the multiple rRNA databases for bacterial, archaeal and eukaryotic sequences [7, 8]. The  
153 non-rRNA reads (ranging from 56 to 73 million) from 24 anammox sludge samples were  
154 mapped to all predicted ORFs of the co-assembled contigs using the read mapper of the CLC  
155 genomics workbench (v6.04, CLCBio, Qiagen) with a mismatch penalty of 2, an  
156 insertion/deletion penalty of 3 and a 95% identity over 90% of the read requirement.

157 The overall gene expression value of a MAG was estimated based on the proportion of recruited  
158 metatranscriptomic reads of all ORFs of given MAG to the all of the reads that mapped to the  
159 ORFs of the recovered 49 MAGs. To estimate relative gene expression of a metabolic pathway  
160 in recovered MAG, relative gene expressions (relativized by median TPM values across all  
161 ORFs within given MAG) of ORFs that involved in given metabolic pathway were averaged  
162 by the identified gene number.

### 163 **S5 Metaproteomic analysis**

164 For the construction of the taxonomy-guided database, protein entries of all the MAGs affiliated  
165 genera/families (Supplementary Table S1) were retrieved from UniprotKB database (protein  
166 sequences were downloaded at March 11, 2018). In addition, a non-redundant gene catalog  
167 predicted genes from the assembled metagenome. The gene catalog was then combined with  
168 the retrieved protein sequences from UniprotKB for database search using MetaPro-IQ  
169 approach as previously described [5].

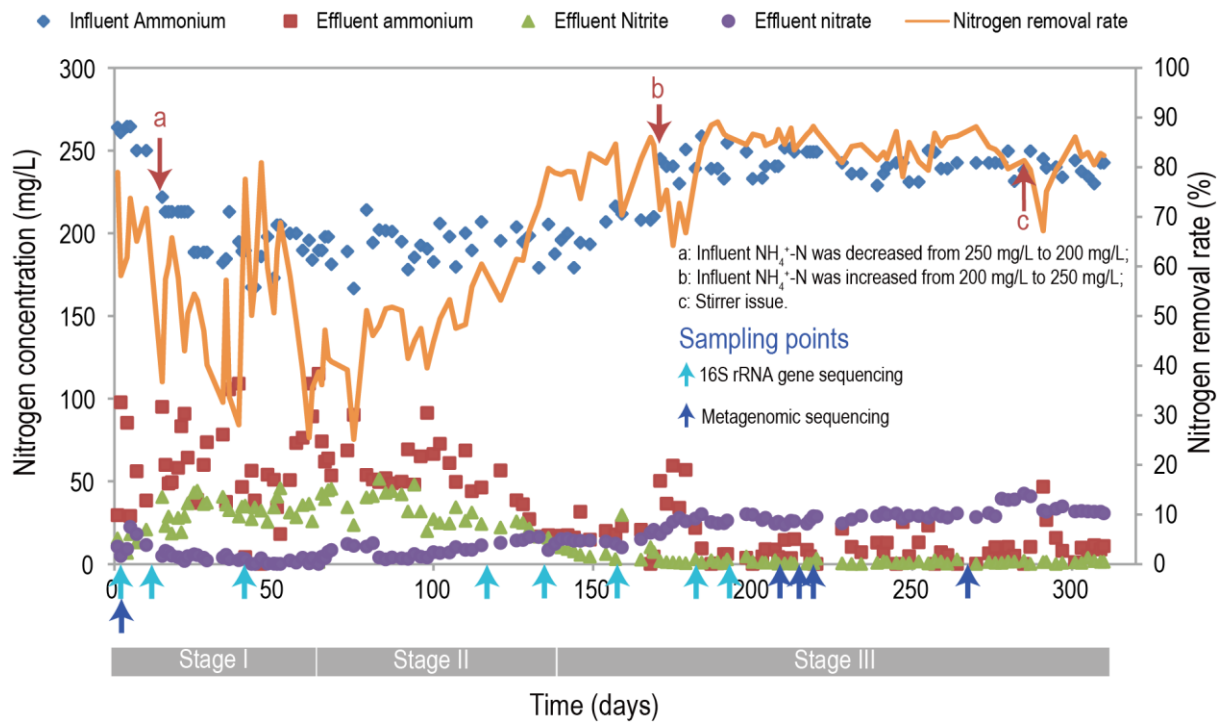
170 Taxonomic and biodiversity analysis of metaproteome data was performed using Unipept [9].  
171 KEGG annotation of the quantified proteins was performed using GhostKOALA [10]. The  
172 KEGG annotation of the leading protein (defined as the top rank protein in a group; the ranking  
173 is based on the number of peptide sequences, the number of PSMs, and the sequence coverage)  
174 in a protein group was used for quantitative analysis. The LFQ intensity of all protein groups  
175 annotated with the same KEGG pathway were summed to represent the pathway abundance.

### 176 **S6 Peptidases identification**

177 The peptidases were identified based on the BLASTP searches against the MEROPS (release  
178 12.0) [11]. The best hits of BLASTP results were filtered and the genes that shared similarity

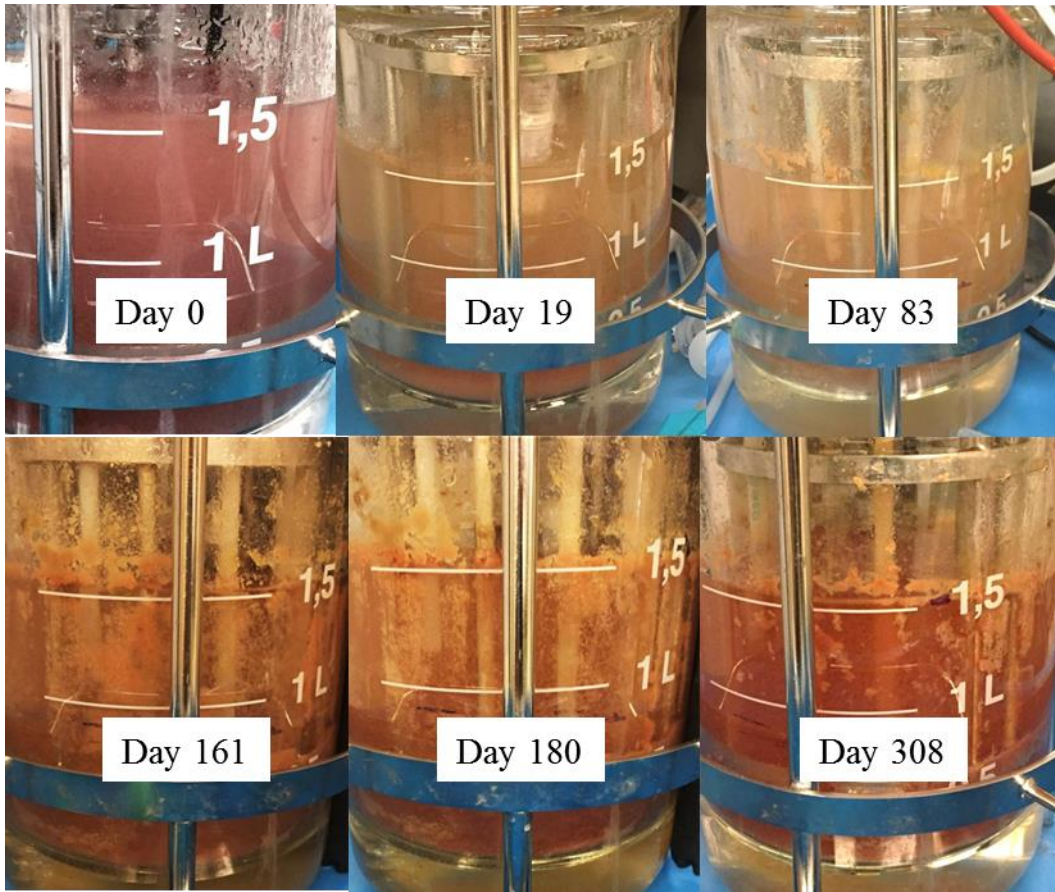
179 at >50% with the database were further extracted to be confirmed using the conserved domain  
180 search (CD-search) [12], and the genes with peptidase domain regions were finally identified  
181 as peptidases.  
182





183

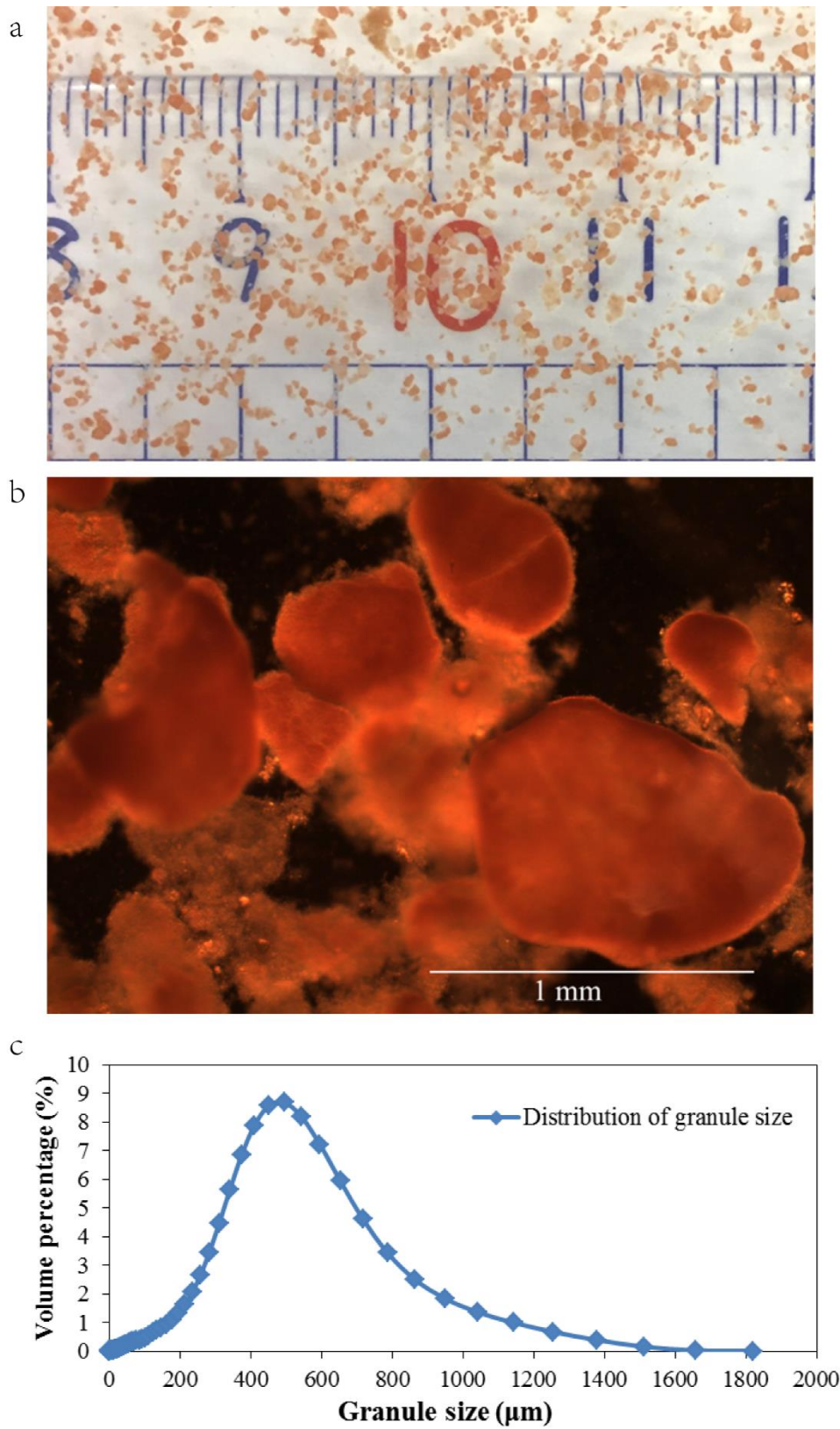
184 Figure S1. Variation of nitrogen components in the influent (ammonium-nitrogen) and effluent  
 185 (ammonium-nitrogen, nitrite-nitrogen and nitrate-nitrogen) and nitrogen removal rate of the  
 186 PNA reactor.



187

188 Figure S2. Color changes of sludge in the studied one-stage PNA reactor.

189

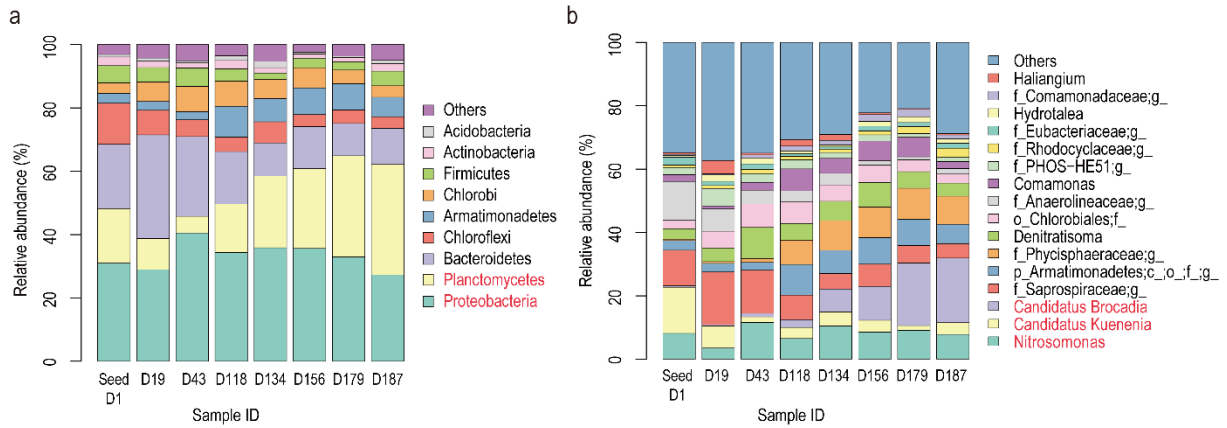


190

191 Figure S3. Characterization of the anammox granules on day 308. a, Image of the anammox

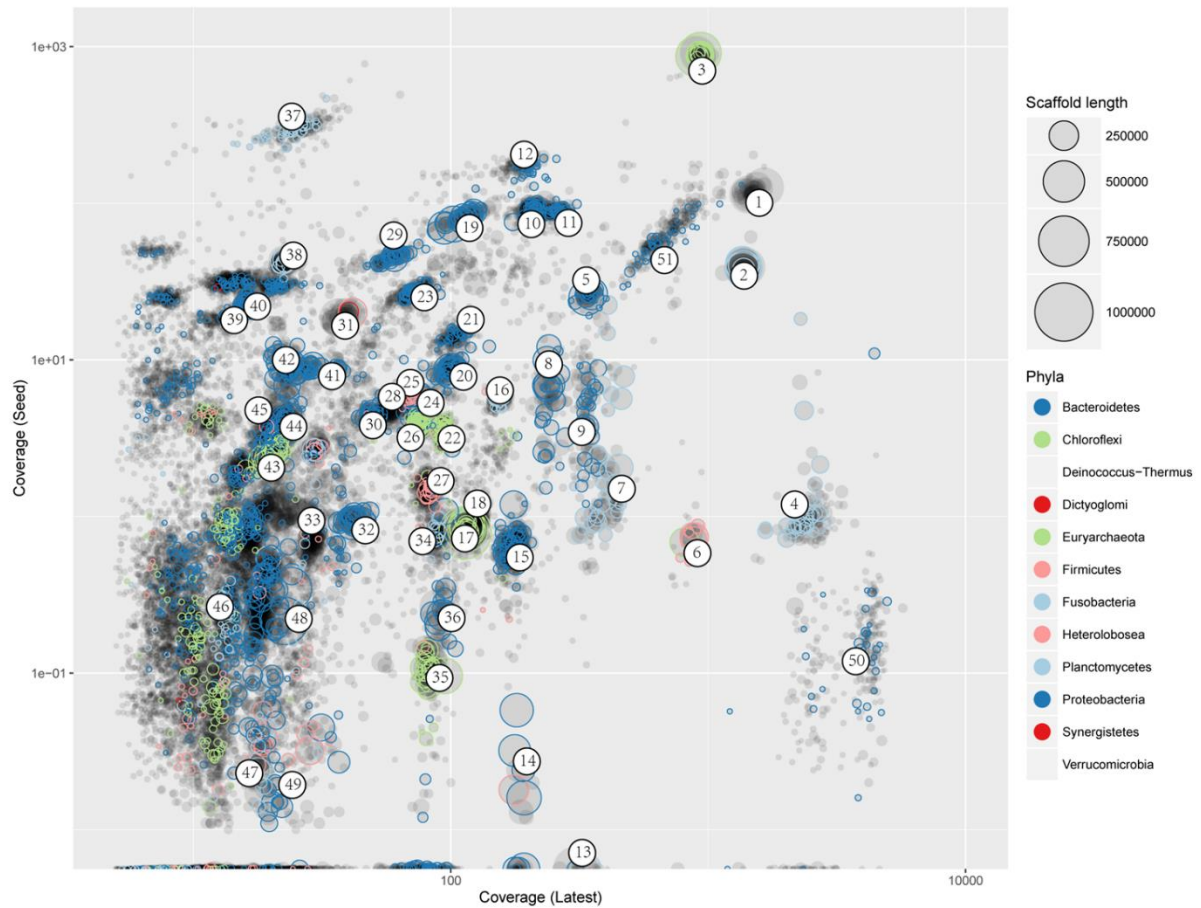
192 granules. b, Light microscope of the anammox granules. c, Size distribution of the anammox

193 sludge.



194

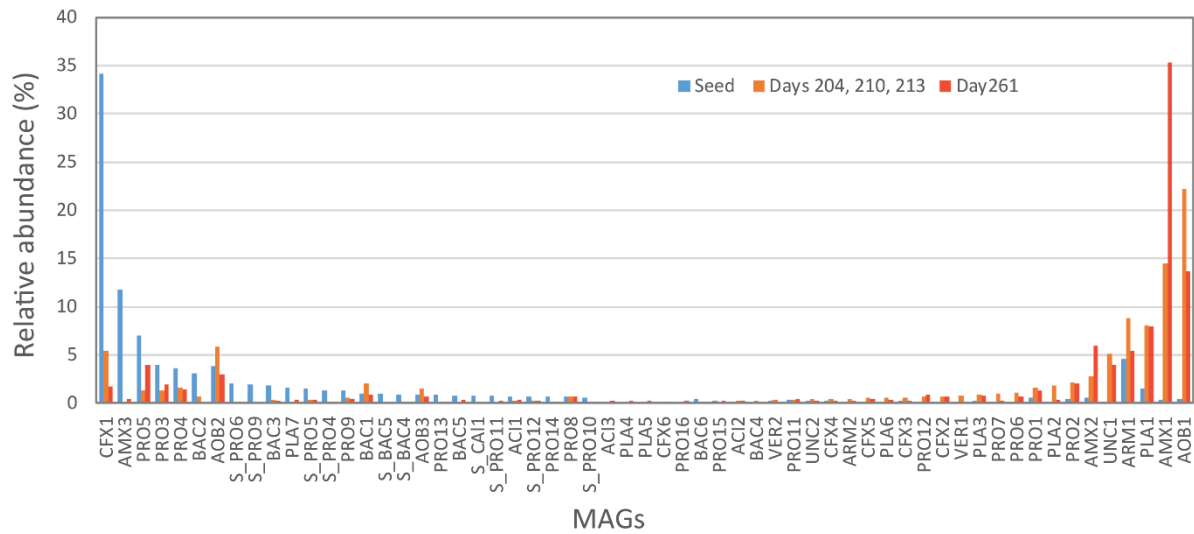
195 Figure S4. Microbial community structures in the anammox sludge samples. The relative  
 196 abundance of taxonomic groups is estimated based on the sequence percentage of the total 16S  
 197 rRNA sequences in each activated sludge sample at phylum (a) and genus levels (b). The genera  
 198 that have relative abundance <1% are assigned to the category of “Others”. The taxonomy was  
 199 presented at the lowest level that can be identified.



200

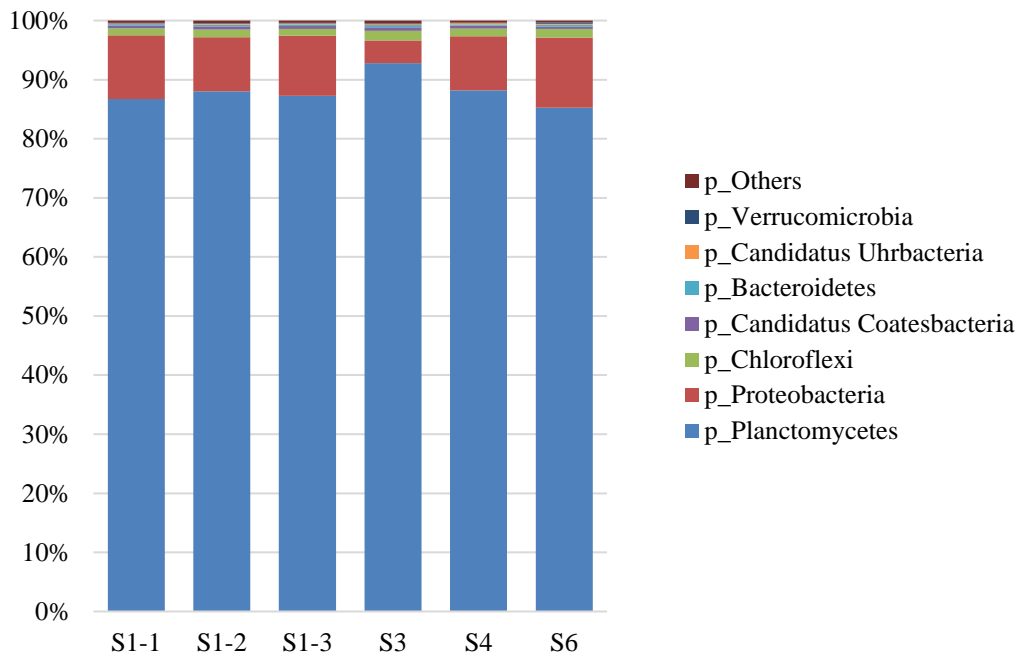
201 Figure S5. Plot of differential coverage binning approach, the corresponding relationships  
 202 between IDs and MAGs information are listed in Table S1. The coverage of x-axis represents  
 203 the mapping coverage of metagenomic data originated from the samples taken on days 204,  
 204 210 and 213, and the y-axis represents the mapping coverage of metagenomic data originated  
 205 from the sample of seed sludge.





206

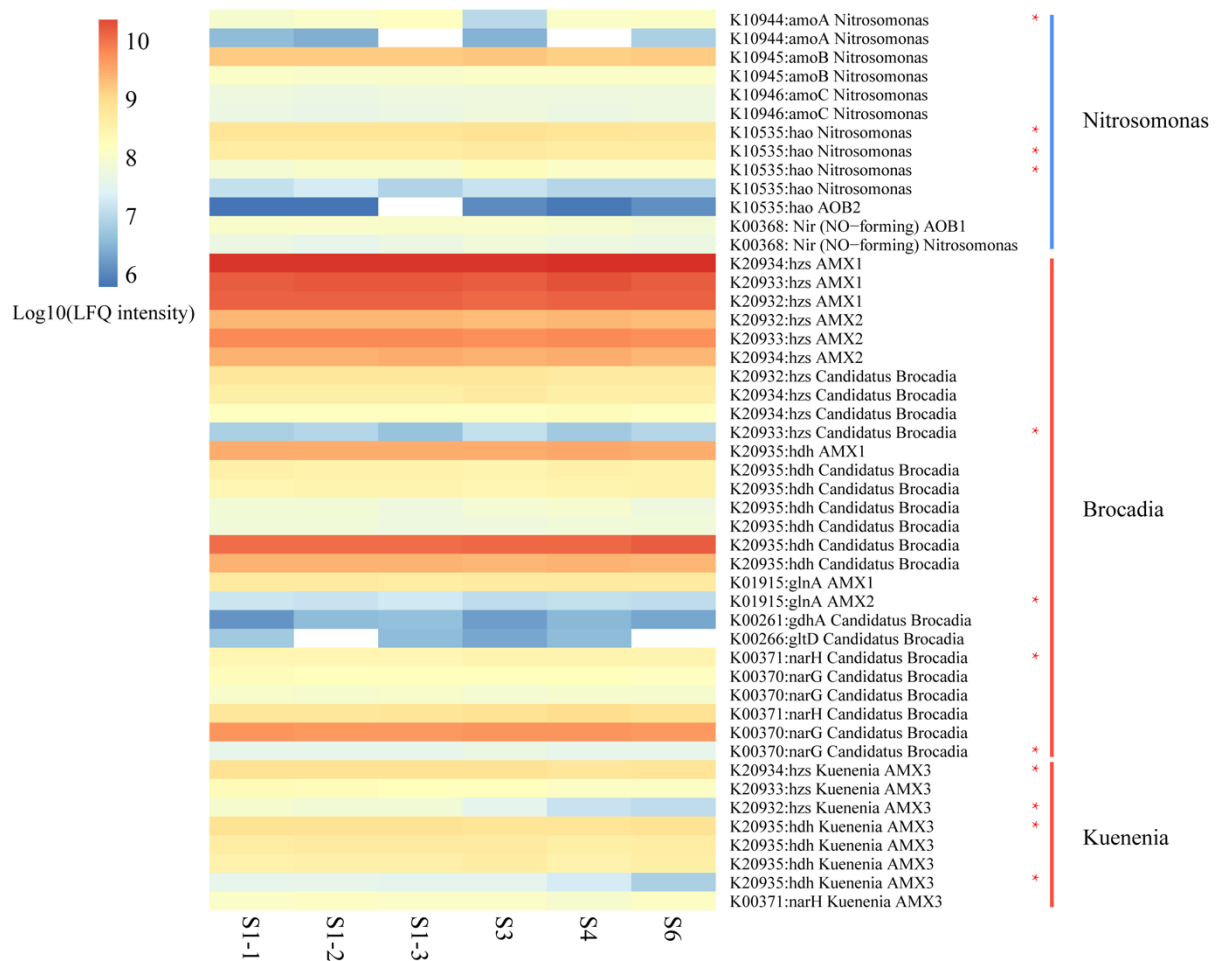
207 Figure S6. Comparison of relative abundance in different anammox sludge samples. The  
 208 relative abundance (normalized by the genome size) represents the ratio of recruited  
 209 metagenomic sequences of one given MAG to the total recruited metagenomic sequences of all  
 210 the recovered MAGs.



211

212 Figure S7. Relative abundance (weighted) of bacterial community composition assessed by  
 213 identified protein. S1-1, S1-2, and S1-3 are the technical repeats of sample S1.

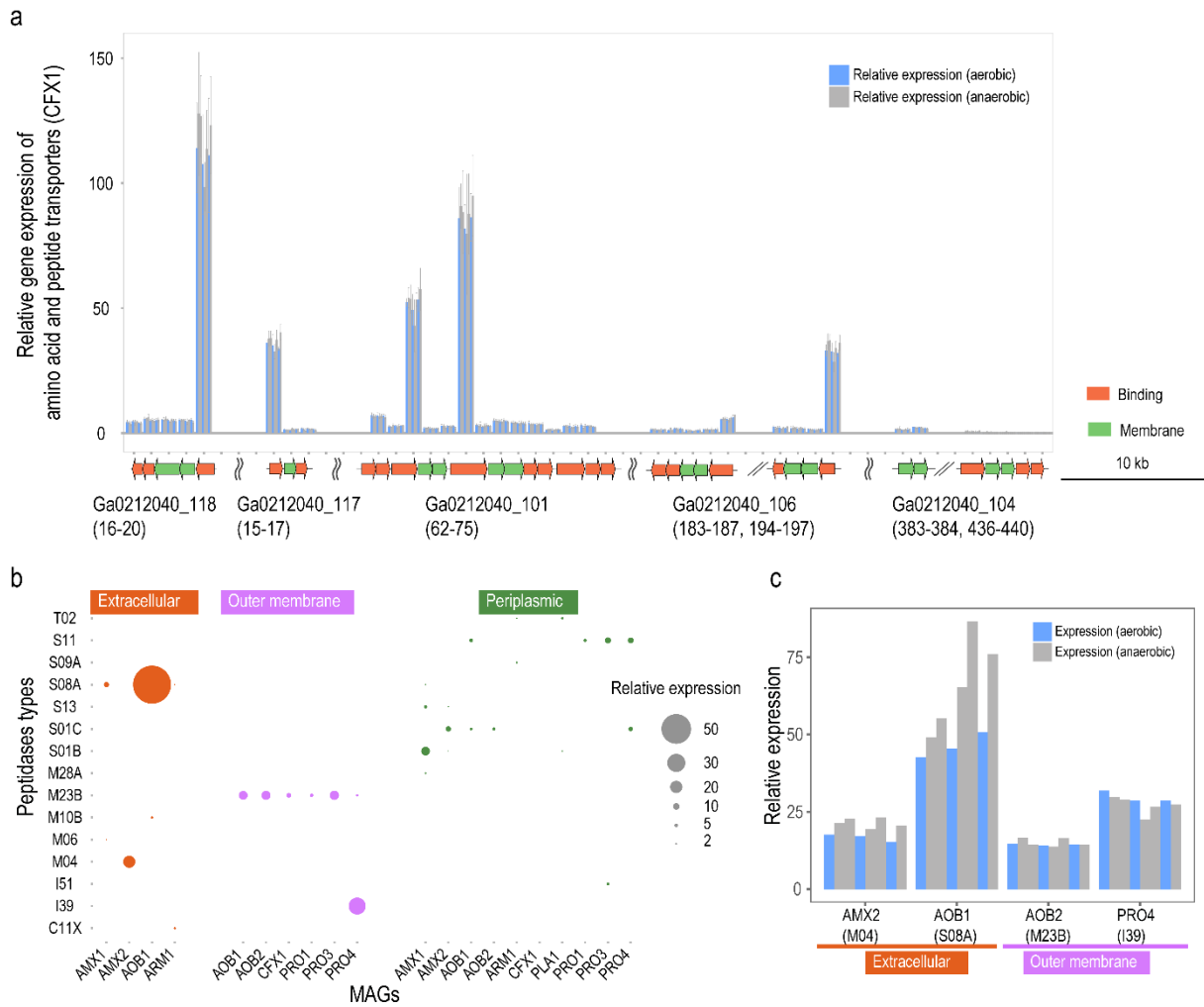
214



215

216 Figure S8. Identified proteins (log10(LFQ intensity)) for nitrogen metabolism in AOB and  
 217 anammox bacteria. Proteins that could be assigned to specific ORFs of recovered MAGs were  
 218 represented with MAG ids, the proteins with best hits to the UniProt database were represented  
 219 with taxonomy (genus level). Differential protein expressions are marked with red asterisk  
 220 (ratio >1.2 or <0.83 coupled with a P value <0.05).

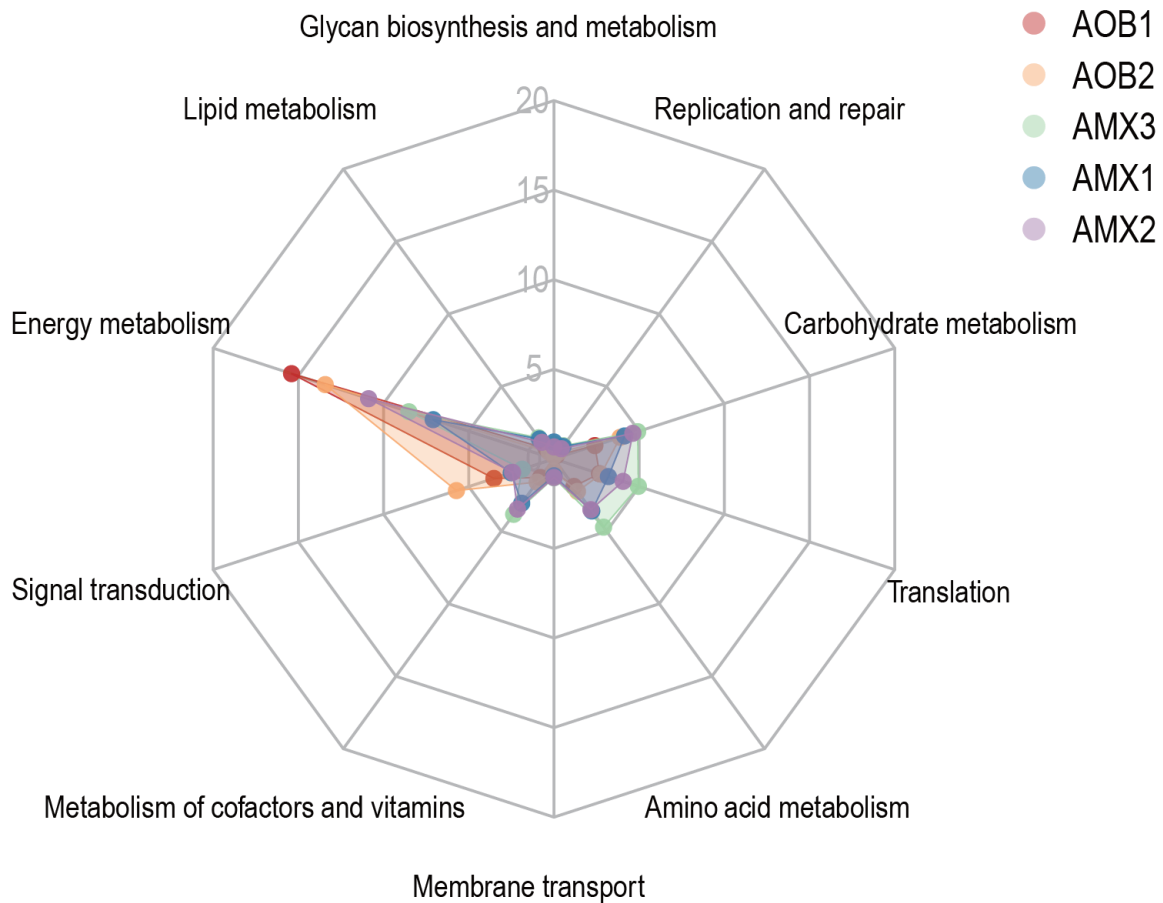




221

222 Figure S9. Relative gene expression of amino acid transporters in CFX1 and identified  
 223 peptidases in dominant organisms. (a) Relative gene expression of amino acid and peptide  
 224 transporters in CFX1 throughout the time series, and aligned with the corresponding gene loci.  
 225 The wiggly lines indicate ends of the contig, and parallel double lines show a break in locus  
 226 organization. Subfamily types of the encoded transporters are represented by color. (b) ORFs  
 227 of dominant organisms (relative abundance >1%) were firstly annotated using MEROPS  
 228 database, and the potential peptidases were further confirmed by CD search. The locations of  
 229 peptidases were predicted by PSORT, and the extracellular, outer membrane and periplasmic  
 230 peptidases are shown in this figure. (c) Dynamics of highly expressed genes throughout the  
 231 time series.

232



233

234 Figure S10. Gene expression profiles of ten selected metabolic pathways in the dominant  
 235 autotrophs. These were estimated based on the ratios of recruited metatranscriptomic sequences  
 236 of genes involved in selected pathways to the total recruited metatranscriptomic sequences of  
 237 the corresponding MAGs.

238

239 **Reference:**

- 240 1. Vangsgaard AK. Modeling, experimentation, and control of autotrophic nitrogen  
241 removal in granular sludge systems. Unpublished doctoral thesis Technical university  
242 of Denmark. 2013.
- 243 2. Liu Y, Niu Q, Wang S, Ji J, Zhang Y, Yang M, Hojo T, Li YY. Upgrading of the symbiosis  
244 of *Nitrosomanas* and anammox bacteria in a novel single-stage partial nitrification-  
245 anammox system: Nitrogen removal potential and Microbial characterization.  
246 *Bioresour Technol.* 2017;244:463-472.
- 247 3. Barr JJ, Dutilh BE, Skennerton CT, Fukushima T, Hastie ML, Gorman JJ, Tyson GW,  
248 Bond PL. Metagenomic and metaproteomic analyses of *Accumulibacter* phosphatis-  
249 enriched floccular and granular biofilm. *Environ Microbiol.* 2016;18:273-287.
- 250 4. Hansen SH, Stensballe A, Nielsen PH, Herbst FA. Metaproteomics: Evaluation of  
251 protein extraction from activated sludge. *Proteomics.* 2014;14:2535-2539.
- 252 5. Zhang X, Ning Z, Mayne J, Moore JI, Li J, Butcher J, Deeke SA, Chen R, Chiang CK,  
253 Wen M, et al. MetaPro-IQ: a universal metaproteomic approach to studying human and  
254 mouse gut microbiota. *Microbiome.* 2016;4:31.
- 255 6. Albertsen M, Hugenholtz P, Skarshewski A, Nielsen KL, Tyson GW, Nielsen PH.  
256 Genome sequences of rare, uncultured bacteria obtained by differential coverage  
257 binning of multiple metagenomes. *Nat Biotechnol.* 2013;31:533-538.
- 258 7. Kopylova E, Noé L, Touzet H. SortMeRNA: fast and accurate filtering of ribosomal  
259 RNAs in metatranscriptomic data. *Bioinformatics.* 2012;28:3211-3217.
- 260 8. Lawson CE, Wu S, Bhattacharjee AS, Hamilton JJ, McMahon KD, Goel R, Noguera  
261 DR. Metabolic network analysis reveals microbial community interactions in anammox  
262 granules. *Nat Commun.* 2017;8:15416.
- 263 9. Mesuere B, Debyser G, Aerts M, Devreese B, Vandamme P, Dawyndt P. The Unipept  
264 metaproteomics analysis pipeline. *Proteomics.* 2015;15:1437-1442.
- 265 10. Kanehisa M, Sato Y, Morishima K. BlastKOALA and GhostKOALA: KEGG tools for  
266 functional characterization of genome and metagenome sequences. *J Mol Biol.*  
267 2016;428:726-731.
- 268 11. Rawlings ND, Barrett AJ, Finn R. Twenty years of the MEROPS database of proteolytic  
269 enzymes, their substrates and inhibitors. *Nucleic Acids Res.* 2015;44:D343-D350.
- 270 12. Marchler-Bauer A, Bryant SH. CD-Search: protein domain annotations on the fly.  
271 *Nucleic Acids Res.* 2004;32:W327-W331.